Exact results on light scattered from atoms pumped by coherent and chaotic fields of arbitrary bandwidth

Gautam Vemuri and Rajarshi Roy
School of Physics, Georgia Institute of Technology, Atlanta, Georgia 30332

G. S. Agarwal
School of Physics, University of Hyderabad, Hyderabad 500134, India
(Received 22 September 1989)

The dynamical behavior of an atom interacting with a coherent field and a chaotic field is studied. Monte Carlo methods are used to integrate the equations describing the dipole moment, population inversion, and two-time correlation functions. The chaotic field can have a finite correlation time. Numerical results for a wide range of the parameters are given. The results depend sensitively on the ratio of the Rabi frequency and the bandwidth of the chaotic field. It is shown how an intense coherent field can suppress the effects of incoherence. The intensity of fluorescence as a function of detuning exhibits narrowing as the strength of the coherent field increases.

INTRODUCTION

Scattering of light by atoms under various pumping conditions[1] has been extensively studied. The spectrum of the emitted radiation is very sensitively dependent on the pumping process. In particular, the stochastic fluctuations of the pump fields affect the spectrum. Various models of pump fluctuations have been treated in the past: these include (a) the phase diffusion model,[2–4] in which only the phase of the field fluctuates and exact analytical solutions are known: (b) the chaotic field model,[5] in which the field's complex amplitude is a two-dimensional Gaussian process, and for which exact solutions have been obtained numerically by using matrix continued fractions; (c) jump models[6,7]—in which amplitude, phase, or frequency is taken to be a discontinuous Markov process. These also lead to exact solutions. The dynamics of an atom excited by a phase fluctuating field have been recently studied experimentally.[8–11] Most previous works deal with the interaction of a single field with the atomic system. Clearly, many situations will involve atomic interaction with a field which has both coherent and incoherent components, i.e., the field interacting with the atom has the form

$$\mathbf{E}=\hat{\varepsilon}[\varepsilon_0+\varepsilon_1(t)]e^{-i\omega_c t+i\mathbf{k}\cdot\mathbf{r}}+\text{c.c.}\ , \tag{1}$$

where ε_0 is the coherent part of the field envelope and ω_c is its optical frequency. The fluctuating part of the field is represented by $\varepsilon_1(t)$. Generally one would expect $\varepsilon_1(t)$ to be chaotic in character; i.e., $\varepsilon_1(t)$ is a two-dimensional Gaussian Markov process with correlation functions

$$\begin{aligned}&\langle \varepsilon_1(t)\varepsilon_1^*(t')\rangle = e^{-\Gamma|t-t'|}\langle \varepsilon_1^2\rangle\ ,\\ &\langle \varepsilon_1(t)\varepsilon_1(t')\rangle = 0\ .\end{aligned} \tag{2}$$

The dynamics of the system depends critically on the correlation time Γ^{-1} of the stochastic component.

THEORY

In this paper we study the scattering of light from a two-level system which is being pumped by both coherent and chaotic fields. In view of the complexity of the system we use Monte Carlo methods to evaluate the steady-state behavior and the spectrum of the scattered field.[12–14] We discuss the spectrum in several interesting regimes of parameter values involved in the problem.

(a) When the correlation time of the stochastic part of the field is very short compared to the radiative lifetime $(2\gamma)^{-1}$, i.e., $\Gamma \gg \gamma$, we show how very interesting line-narrowing effects arise as the Rabi frequency of the driving field becomes much larger than Γ. Note further that as long as Γ is much larger than all other time scales in the problem, the usual Mollow spectrum is obtained.

(b) When the correlation time is comparable to the radiative lifetime, the spectral features are very different from what one might expect on the basis of Bloch equations.

(c) The effect of detuning the field; we study how the asymmetries of the spectra depend on various parameters.

The dynamics of the two-level atom with frequency ω_0 in the presence of the pumping field is given by the density-matrix equation[1]

$$\frac{\partial\rho}{\partial t}=\frac{i}{\hbar}\left[\left(\frac{\mathbf{d}\cdot\hat{\varepsilon}}{\hbar}[\varepsilon_0+\varepsilon_1(t)]S^+ +\text{H.c.}\right),\rho\right] -i\Delta[S^z,\rho]-\gamma(S^+S^-\rho-2S^-\rho S^+ +\rho S^+S^-)\ . \tag{3}$$

Here ρ is in a frame rotating with the frequency ω_c of the field. The phase factor $(e^{-i\mathbf{k}\cdot\mathbf{r}})$ has been absorbed in the definition of d. Δ is the detuning parameter $(\omega_0-\omega_c)$. The spontaneous emission from the excited state to the ground state is represented by the last pair of parentheses in Eq. (3). Let Ω be the Rabi frequency associated with the coherent part of the field

 ©1990 The American Physical Society

$$\Omega=\frac{2\mathbf{d}\cdot\hat{\boldsymbol{\varepsilon}}}{\hbar}\varepsilon_0 \tag{4a}$$

and let β be the parameter defined by

$$\beta=\frac{2}{\Gamma}\langle x(t)x^*(t')\rangle , \tag{4b}$$

where $x(t)$ is given by

$$x(t)=\frac{\mathbf{d}\cdot\hat{\boldsymbol{\varepsilon}}}{\hbar}\varepsilon_1(t) . \tag{4c}$$

The Bloch equations for the mean values of the dipole moment operators S^+ and S^- and the inversion operator S^z are given by

$$\dot{\psi}=\begin{bmatrix}\langle S^+\rangle\\ \langle S^-\rangle\\ \langle S^z\rangle\end{bmatrix}=C_0\psi-ix(t)C_+\psi-ix^*(t)C_-\psi+g , \tag{5}$$

where

$$C_0=\begin{bmatrix}-\gamma+i\Delta & 0 & -i\Omega\\ 0 & -\gamma-i\Delta & i\Omega\\ \frac{-i\Omega}{2} & \frac{i\Omega}{2} & -2\gamma\end{bmatrix} , \tag{6a}$$

$$C_+=\begin{bmatrix}0&0&0\\0&0&-2\\1&0&0\end{bmatrix} ,$$

$$C_-=\begin{bmatrix}0&0&2\\0&0&0\\0&-1&0\end{bmatrix} , \quad g=\begin{bmatrix}0\\0\\-\gamma\end{bmatrix} . \tag{6b}$$

Note that the Bloch equations for the ψ's are really Langevin equations with stochastic modulation appearing in multiplicative form. In what follows, such equations will be integrated using Monte Carlo methods to get the dynamical behavior of the system. We also note that if the correlation time Γ^{-1} goes to zero, then stochastic averaging over $x(t)$ can be carried out with the result

$$\langle\dot{\psi}\rangle=\left[C_0-\frac{\beta}{2}C_+C_--\frac{\beta}{2}C_-C_+\right]\langle\psi\rangle+g , \tag{7}$$

where β is defined by (4b). Clearly, in such a case we have the standard optical Bloch equations with transverse and longitudinal relaxation constants defined by

$$\frac{1}{T_1}=2(\gamma+\beta)=\frac{2}{T_2} . \tag{8}$$

We next introduce the correlation matrix $R(t+\tau,t)$ defined by

$$R(t+\tau,t)=\begin{bmatrix}\langle S^+(t+\tau)S^-(t)\rangle\\ \langle S^-(t+\tau)S^-(t)\rangle\\ \langle S^z(t+\tau)S^-(t)\rangle\end{bmatrix} . \tag{9}$$

The correlation matrix R obeys an equation that can be obtained from (5) and the quantum regression theorem

$$\frac{dR}{d\tau}=C_0R(t+\tau,t)-i[x(t+\tau)C_++x^*(t+\tau)C_-]R(t+\tau,t)+g\langle S^-(t)\rangle . \tag{10}$$

The set of equations (10) is in the form of Langevin equations because of the stochastic field $x(t)$. The spectrum of the scattered field is defined by

$$S(\omega)=\mathrm{Re}\int_0^\infty d\tau[\langle\langle S^+(t+\tau)S^-(t)\rangle\rangle-\langle\langle S^+(t+\tau)\rangle\rangle\langle\langle S^-(t)\rangle\rangle]e^{-i(\omega-\omega_c)\tau} \tag{11}$$

$$=\mathrm{Re}\int_0^\infty d\tau\, e^{-i(\omega-\omega_c)\tau}(\langle R_1\rangle-\langle\psi_1\rangle\langle\psi_2\rangle) , \tag{12}$$

where the second angular bracket denotes the ensemble average with respect to the fluctuations of the field $x(t)$. Thus, in order to get the spectrum, the sets of equations (5) and (10) are integrated numerically using Monte Carlo techniques.

MONTE CARLO SIMULATIONS

We represent the complex, stochastic field $x(t)$ by exponentially correlated (colored) Gaussian noise, with the properties

$$\langle x(t)\rangle=0 \tag{13a}$$

and

$$\langle x(t)x^*(t')\rangle=\frac{\Gamma\beta}{2}e^{-\Gamma|t-t'|} , \tag{13b}$$

where Γ is the inverse of the correlation time and $(\Gamma\beta/2)$ is the variance of $x(t)$. This noise has a Lorentzian spectral profile with a full width at half maximum (FWHM) equal to 2Γ.

The algorithm used to generate $x(t)$ is detailed in Ref. 15 and is briefly described here. We first outline a method for producing Gaussian δ-correlated (white) noise g_w. This noise has the well-known properties

$$\langle g_w(t)\rangle=0, \quad \langle g_w(t)g_w^*(t')\rangle=\beta\delta(t-t') , \tag{14}$$

which completely determine all its statistical properties. It is easily produced by the Box-Mueller algorithm:

$$g_w=[-\beta\Delta t\ln(a)]^{1/2}\exp(2\pi ib) , \tag{15}$$

where a and b are computer-generated, uniformly distributed random numbers between 0 and 1.

Exponentially correlated colored noise as described in Eq. (13) is obtained from the equation

$$\dot{x}=-\Gamma x+\Gamma g_w \tag{16}$$

in which g_w is still Gaussian white noise as defined before. It has been shown previously[15] that by integrating the above equation (16) we get

$$x(t+\Delta t)=x(t)e^{-\Gamma\Delta t}+h(t)\ , \tag{17}$$

where h depends on g_w and is Gaussian with zero mean and a second moment given by

$$\langle |h(t,\Delta t)|^2\rangle = \frac{\Gamma\beta}{2}(1-e^{-2\Gamma\Delta t})\ . \tag{18}$$

Thus to generate the colored noise $x(t)$, we first produce h by the formula

$$h=[-0.5\beta\Gamma(1-e^{-2\Gamma\Delta t})\ln(a)]^{1/2}\exp(2\pi i b)\ , \tag{19}$$

where, as before, a and b are computer-generated, uniformly distributed random numbers between 0 and 1. The exponentially correlated noise is then obtained from expression (17).

The three Langevin equations (5) were solved numerically using the colored noise generated above. An Euler method was used for the numerical stochastic integration with a time step of 0.001. Integration over 10 000 steps was carried out to reach a final dimensionless time of 10

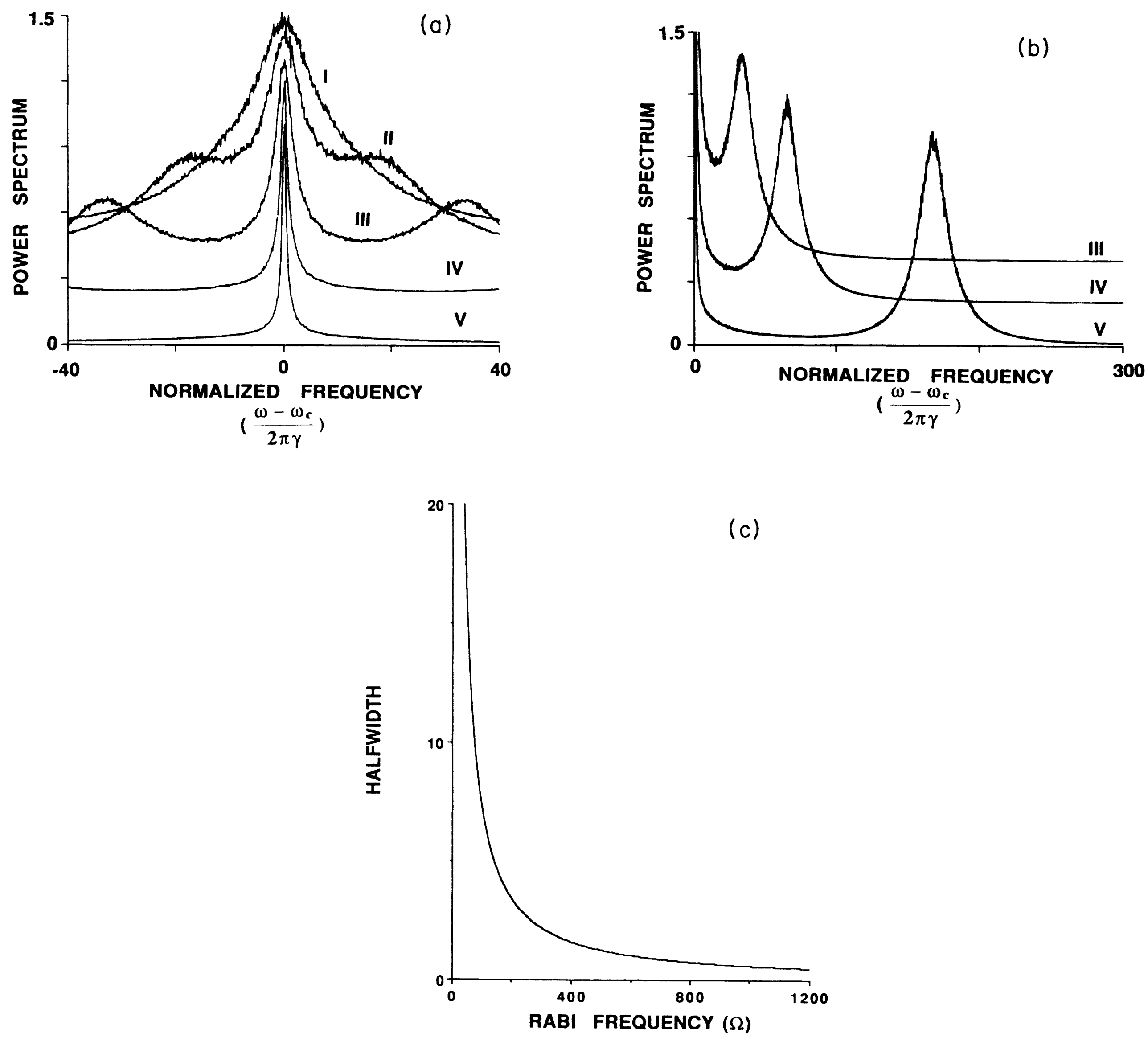

FIG. 1. (a) The spectrum of fluorescence as a function of normalized frequency $(\omega-\omega_c)2/\pi\gamma$ for $\beta=20\gamma$, $\Gamma=100\gamma$ and for Rabi frequency (Ω) of the coherent pump equal to (I) 40γ, (II) 100γ, (III) 200γ, (IV) 400γ, and (V) 1000γ. The central peak shows dramatic narrowing. For clarity, the origin on the y axis is shifted for curves (I)–(IV) by 0.5, 0.4, 0.3, and 0.2 units, respectively. (b) Sidebands of the fluorescence spectrum for Ω/γ of 200, 400, and 1000. Curves (III) and (IV) are shifted by 0.4 and 0.2 units for clarity. (c) Half-width of the central component as a function of the Rabi frequency for $\beta=20\gamma$ and $\Gamma=100\gamma$. The narrowing is very clearly depicted here.

units. The values of $\langle S^-(t)\rangle$ were used as the initial condition for the next set of three Langevin equations (10). Once again a time step of 0.001 was chosen for the numerical integration and 10 000 steps was carried out to obtain the elements of the correlation matrix R. A fast Fourier transform of $\langle R_1(\tau)\rangle$ gave the power spectrum $S(\omega)$ as described in (12). An averaging of the power spectrum over 1000 trajectories obtained with different initial values of $\langle S^-(t)\rangle$ was performed.

RESULTS

In this section we describe the results for power spectra of the scattered light when an electric field with a

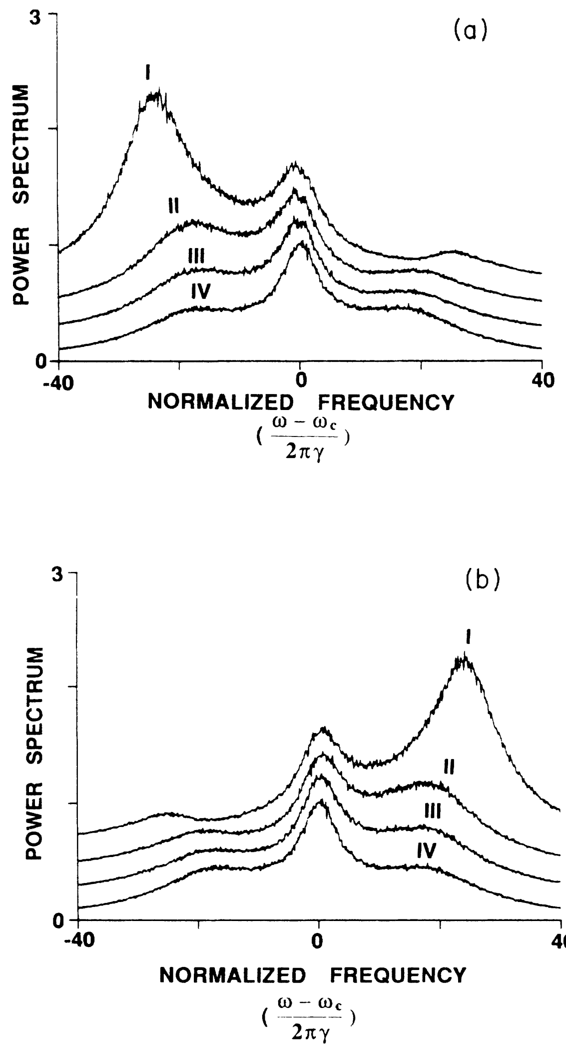

FIG. 2. (a) Effect of detuning on spectrum for $\beta=20\gamma$, $\Gamma=100\gamma$, and $\Omega=100\gamma$. Curves (I)–(IV) are for Δ of 50γ, 20γ, 10γ, and 0, respectively. The spectra show a strong asymmetry, with the left sidebands becoming more pronounced. Curves are offset by 0.6, 0.4, and 0.2 units on the y axis. (b) Effect of negative detuning on spectrum. β, Γ, and Ω same as for (a). Curves (I)–(IV) are for Δ of -50γ, -20γ, -10γ, and 0. The asymmetry is switched, with the right sidebands becoming more prominent. Curves offset by 0.6, 0.4, and 0.2 units on the y axis.

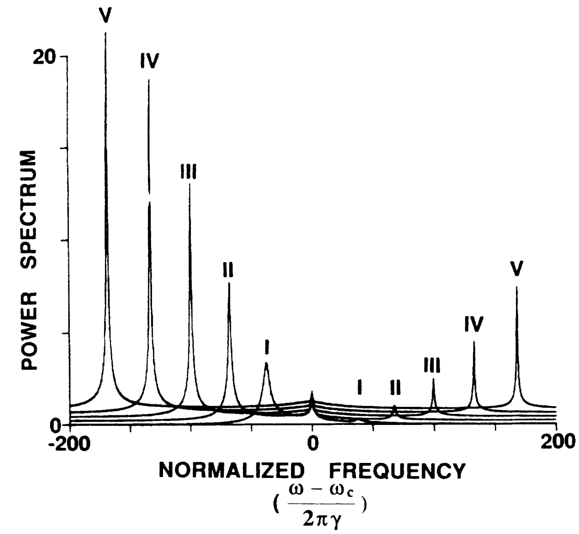

FIG. 3. Spectra for detunings larger than Ω. Curves (I)–(V) are for detunings of 100γ, 200γ, 300γ, 400γ, and 500γ. $\beta=20\gamma$, Γ and Ω are 100γ. Curves (II)–(V) are offset by 0.2, 0.3, 0.4, and 0.5 units on the y axis.

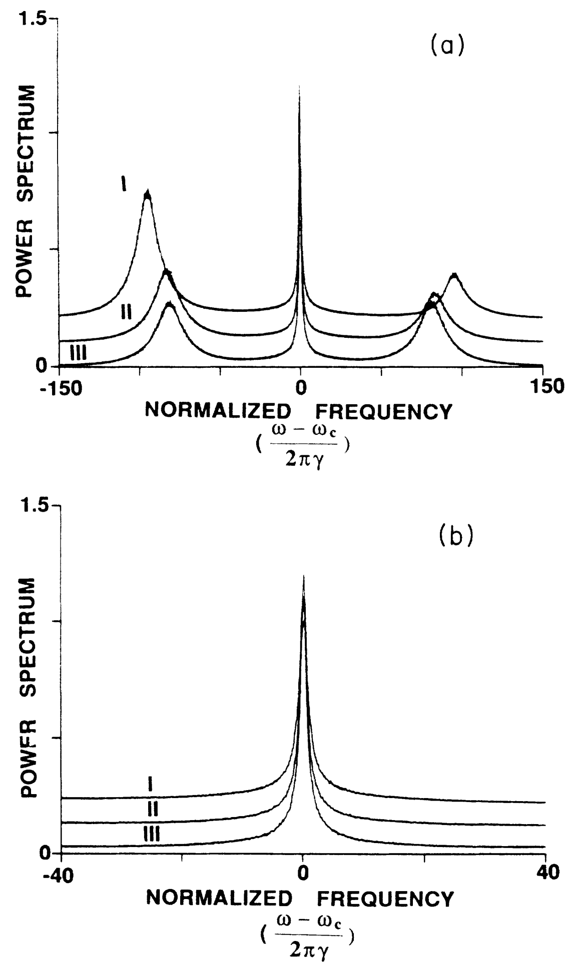

FIG. 4. (a) Spectra for $\Omega>\Gamma$. Curves (I)–(III) are for $\beta=20\gamma$, $\Gamma=100\gamma$, $\Omega=500\gamma$, and Δ of 150γ, 50γ, and 0. Curves (I) and (II) are offset by 0.2 and 0.1 units on the y axis. (b) Central peaks of (a) on an expanded scale.

coherent and a stochastic component interacts with a two-level atom. The sensitive dependence of the results on the ratio of the Rabi frequency and the bandwidth of the chaotic field is shown. We first consider the case when the correlation time $(1/\Gamma)$ of the stochastic amplitude is short compared to γ^{-1}, i.e., $\Gamma \gg \gamma$. In Fig. 1(a) we show how the spectrum of the scattered light changes as the intensity of the coherent component is increased. For values of Ω, low compared to Γ, but large compared to $(\gamma+\beta)$ we recover Mollow's three-peak spectrum, i.e., we find peaks centered at $\omega=\omega_c$ with a width $(\gamma+\beta)$ and two sidebands at $\omega=\omega_c\pm\Omega$ with widths $\frac{3}{2}(\gamma+\beta)$. This is because in this limit the optical Bloch equations hold. As Ω becomes larger than Γ, the usual optical Bloch description cannot be used. This is because within the correlation time of the stochastic field, several Rabi oscillations due to the coherent component are possible. This leads to extreme narrowing of the central component.[16] In fact, the central component narrows from a half-width of $(\gamma+\beta)$ to γ. [The sidebands are shown in Fig. 1(b).] We suggest the following experiment for the verification of this result. First irradiate a two-level atom with a wide-band chaotic field and measure the spectrum of the scattered radiation. Next, apply a coherent field of varying intensity in addition to the wide-band chaotic field and study the spectrum to compare with our predicted results. The experimental measurements should be similar to the results shown in Fig. 1(c).

A situation of considerable interest would be the detuning of the electric field from the resonant frequency of the two-level atom. In Fig. 2 is shown the effect of detuning the field. We choose Ω comparable to $\Gamma \gg \gamma$. The

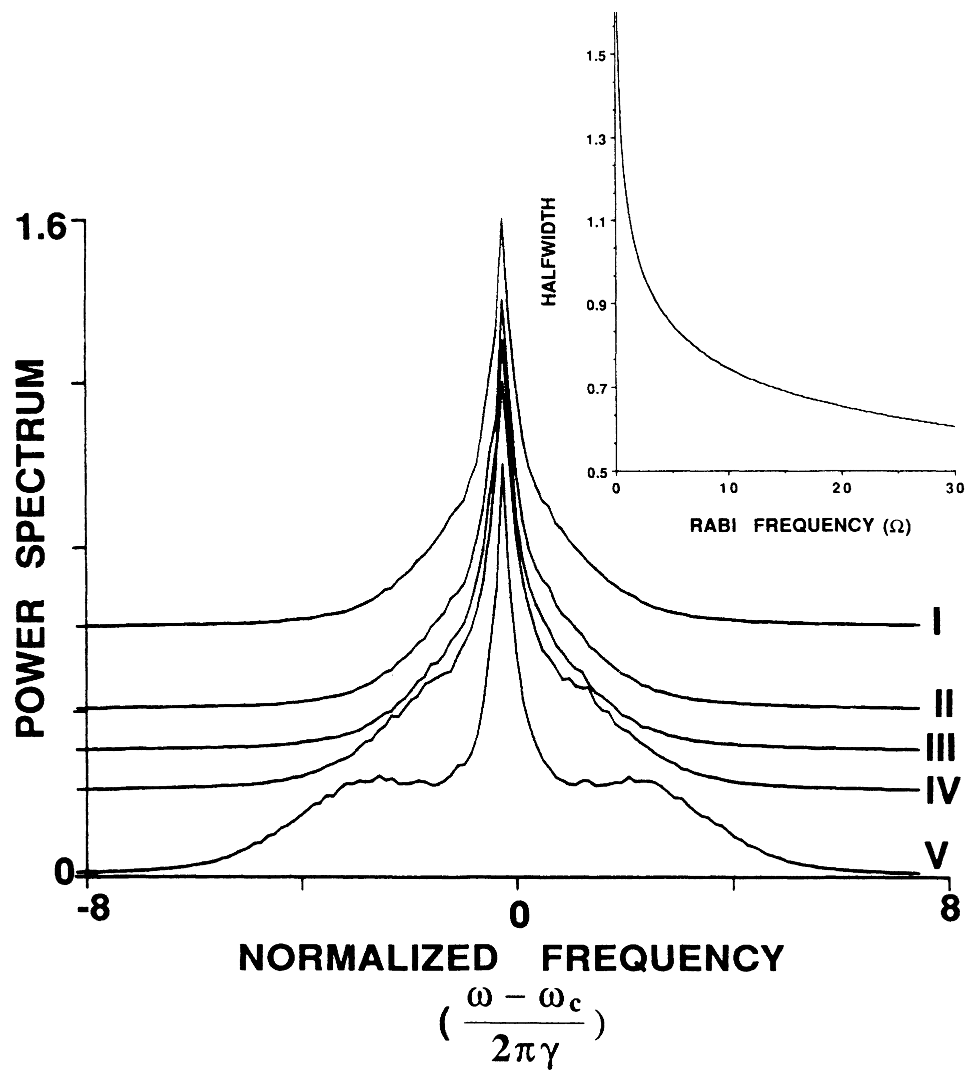

FIG. 5. Spectra for longer correlation time, $\Gamma=\gamma$ and $\beta=20\gamma$. Curves (I)–(V) are for Ω/γ of 0.2, 1, 2, 10, and 20. Curves (I)–(IV) are offset by 0.6, 0.4, 0.3, and 0.2 units on the y axis. Inset shows half-width of the central component vs Rabi frequency for $\Gamma=\gamma$.

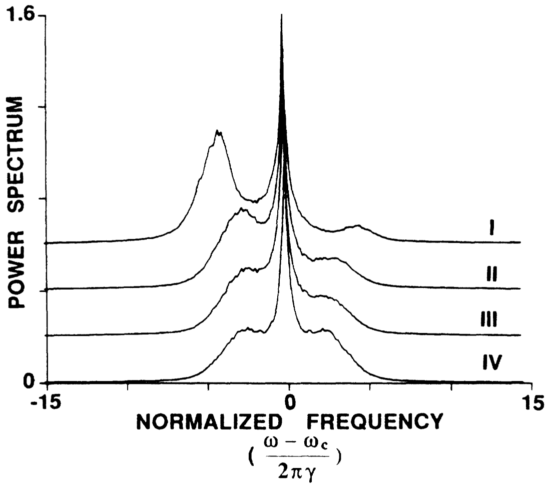

FIG. 6. Effect of detuning on spectra for $\beta=20\gamma$, $\Gamma=\gamma$, and $\Omega=20\gamma$. Curves (I)–(IV) are for Δ of 10γ, 4γ, 2γ, and 0. Note the increasing prominence of the left sidebands.

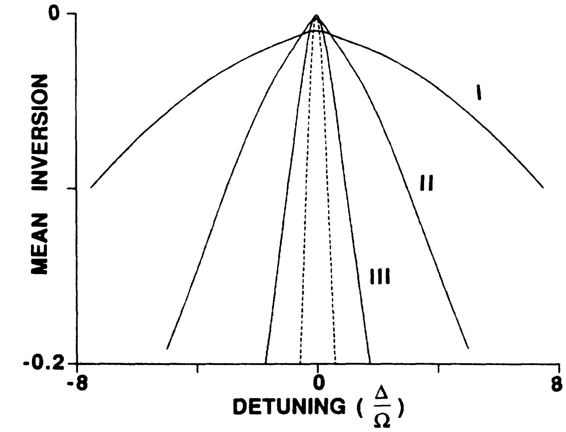

FIG. 7. Mean inversion as a function of the detuning for $\beta=20\gamma$ and $\Gamma=100\gamma$. Curves (I)–(III) are for Ω/γ of 40, 100, and 300. The dashed curve is for a pure, coherent field. Width of the curve narrows with increase in Rabi frequency.

three-photon sideband becomes more and more pronounced as the detuning increases. Figures 2(a) and 2(b) also show the effect of reversing the sign of Δ. We note that reversing the sign of the detuning switches the asymmetry in the spectra. Figure 3 shows the spectrum in the limit of much larger values of the detunings. Note the considerable amplification of the three-photon sideband. In Fig. 4 we give the spectra in the limit $\Omega > \Gamma$, i.e., when several Rabi oscillations are possible within the correlation time of the chaotic field. Figure 4(b) shows the central peaks in Fig. 4(a) on an expanded scale.

We next consider the case when the correlation time of the stochastic field is comparable to the radiative lifetime. In Fig. 5 we show the corresponding spectra for a range of the values of the intensity of the coherent driving field. Curve I is for low values of the coherent field. It effectively gives the spectrum in the presence of the chaotic field alone. The side peak is missing even though the Rabi frequency of the chaotic field is equal to $2\sqrt{10}$. The side peaks start appearing as the coherent part of the field increases.[17] Once again, a narrowing of the central component is observed. This suggests that this narrowing with increase in the intensity of the coherent component is a very general feature. This narrowing aspect is depicted in the inset of Fig. 5 where the half-width of the central component is shown as a function of the intensity of the coherent component. The effect of detuning is shown in Fig. 6. The left sideband again becomes more prominent for positive detunings.

Finally in Fig. 7 we show how the average inversion $\langle\langle S^z\rangle\rangle$ depends on the detuning.[18,19] Note that the intensity I of the scattered light is proportional to $(\frac{1}{2}+\langle\langle S^z\rangle\rangle)$. Results are shown for the case of Γ equal to 100γ and Ω of 40γ, 100γ, and 300γ. As expected, an increase in the Rabi frequency leads to an increase in the mean value of the inversion at resonance, which tends to zero asymptotically. Further, we note that as Ω increases, the width of the average inversion versus (Δ/Ω) curve narrows. This is a very interesting result. In the limit where the usual Bloch equation treatment is valid the width of the inversion versus (Δ/Ω) plot would be independent of the Rabi frequency. But for the model presented in this paper, we find the width decreases with increasing Rabi frequency. The limit of this narrowing is the dashed curve, which is for the case of a pure coherent field. Obviously, the incoherent component causes a broadening of the inversion versus (Δ/Ω) curve.

ACKNOWLEDGMENTS

One of us (G.S.A.) is grateful to the International Division of the National Science Foundation for making available two grants which made this collaboration possible. He is also indebted to Professor J. Cooper for discussions and to the Department of Science and Technology, Government of India for partial support. G.V. and R.R. acknowledge support from the U.S. Department of Energy, Office of Basic Energy Science, Chemical Sciences Division.

[1]B. R. Mollow, Phys. Rev. **188**, 1969 (1969); in *Progress in Optics*, edited by E. Wolf (North-Holland, Amsterdam, 1981), Vol. 19, p. 1.

[2]G. S. Agarwal, Phys. Rev. Lett. **37**, 1383 (1976); Phys. Rev. A **18**, 1490 (1978).

[3]J. H. Eberly, Phys. Rev. Lett. **37**, 1387 (1976); K. Wodkiewicz, Phys. Rev. A **19**, 1686 (1979).

[4]H. J. Kimble and L. Mandel, Phys. Rev. A **15**, 689 (1977).

[5]A. T. Georges, P. Lambropoulos, and P. Zoller, Phys. Rev. Lett. **42**, 1609 (1979); A. T. Georges, Phys. Rev. A **21**, 2034 (1980); P. Zoller, in *Multiphoton Processes*, edited by P. Lambropoulos and S. J. Smith (Springer-Verlag, Berlin, 1986).

[6]G. S. Agarwal, Z. Phys. B **33**, 111 (1979).

[7]B. W. Shore, J. Opt. Soc. Am. B **1**, 176 (1984); K. Wodkiewicz,

B. W. Shore, and J. H. Eberly, Phys. Rev. A **30**, 2390 (1984); a fairly general phase jump model has been recently introduced by A. G. Kofman, R. Zaibel, A. M. Levine, and Y. Prior [Phys. Rev. Lett. **61**, 251 (1988)], who studied the spectrum of resonance fluorescence.

[8]M. W. Hamilton, D. S. Elliot, K. Arnett, S. J. Smith, M. Dziemballa, and P. Zoller, Phys. Rev. A **36**, 178 (1987).

[9]M. W. Hamilton (unpublished).

[10]D. S. Elliot, M. W. Hamilton, K. Arnett, and S. J. Smith, Phys. Rev. A **32**, 887 (1985).

[11]K. Arnett R, Ryan, M. W. Hamilton, J. Brandenberger, T. Bergeman, H. Metcalf, and S. J. Smith (unpublished).

[12]G. S. Agarwal and P. Anantha Lakshmi [Phys. Rev. A **35**, 3152 (1987)] studied the effect of a two-mode field with phase fluctuations on the scattering from a two-level atom.

[13]In a recent paper G. S. Agarwal and S. Singh [Phys. Rev. A **39**, 2239 (1989)] investigated *analytically* the case when the stochastic part ε_1 can be modeled as a two-state jump process. This model leads to interesting predictions on the line narrowing due to a strong coherent field acting on the system.

[14]A. W. McCord [Ph.D. thesis, University of Otago, New Zeland (1989)] has developed matrix continued-fraction methods to treat the dynamics of the atom in the presence of coherent and chaotic fields.

[15]R. F. Fox, I. R. Gatland, R. Roy, and G. Vemuri, Phys. Rev. A **38**, 5938 (1988).

[16]This kind of narrowing was first reported in Ref. 13 where the stochastic field was modeled as a jump process. The present work suggests that the narrowing is a general feature as long as $\Omega \gg \Gamma$.

[17]The spectra in this limit are quite sensitive to the model of the stochastic field as can be seen from the comparison of Fig. 5 with Fig. 2 of Ref. 13. This also suggests that if one had made a decorrelation approximation for the chaotic field, then one would have obtained a very poor result. This is because the mathematical equations for a chaotic field under the decorrelation approximation are identical to those for the jump model of Ref. 13.

[18]Th. Haslwanter, H. Ritsch, J. Cooper, and P. Zoller [Phys. Rev. A **38**, 5652 (1988)] have calculated fluctuations in the radiated intensity by a macroscopic system. These fluctuations result from the fluctuations of the pump field; M. Anderson, R. Jones and S. J. Smith (unpublished) have measured the fluctuations in the radiated intensity. The Monte Carlo method can also be applied to calculate these fluctuations.

[19]Applications of Monte Carlo techniques to four-wave mixing in incoherent fields will be presented elsewhere.